Reexamination of the ground-state Born-Oppenheimer Yb_2 potential

Giorgio Visentin,[1,*] Alexei A. Buchachenko,[1,2,†] and Paweł Tecmer[3,‡]

[1]*Skolkovo Institute of Science and Technology, Skolkovo Innovation Center, Moscow 121205, Russia*

[2]*Institute of Problems of Chemical Physics, RAS, Chernogolovka, Moscow Region 142432, Russia*

[3]*Institute of Physics, Faculty of Physics, Astronomy and Informatics, Nicolaus Copernicus University in Toruń, Grudziadzka 5, 87-100 Torun, Poland*

(Received 8 August 2021; revised 17 October 2021; accepted 28 October 2021; published 10 November 2021)

The precision of the photoassociation spectroscopy of the Yb dimer in degenerate gases is enough to improve the constraints on short-range gravitylike forces if the theoretical knowledge of the Born-Oppenheimer interatomic potential and non-Born-Oppenheimer interactions is refined [Borkowski *et al.*, Sci. Rep. **9**, 14807 (2019)]. The ground-state interaction potential of the ytterbium dimer is investigated at the exact two-component core-correlated coupled-cluster method with singles, doubles, and noniterative triples [CCSD(T)] level of *ab initio* theory in the complete-basis-set limit with extensive augmentation by diffuse functions. For the small basis set the comparison is made with the four-component relativistic finite-nuclei CCSD(T) calculations to identify the contraction of the dimer bond length as the main unrecoverable consequence of the scalar-relativistic approximation. The empirical constraint on the number of bound vibrational energy levels of the $^{174}Yb_2$ dimer is accounted for by representing the global *ab initio*–based Born-Oppenheimer potential with the model semianalytical function containing the scale and shift parameters. The results support the previous evaluation of the Yb dimer potentials from the photoassociation spectroscopy data and provide an accurate and flexible reference for future refinement of the constraints on short-range gravitylike forces by ultracold atomic spectroscopy.

DOI: 10.1103/PhysRevA.104.052807

I. INTRODUCTION

Recent advances in ultracold atomic physics have brought the weakly bound ytterbium dimer, which has never been detected spectroscopically at room temperature, to the forefront of fundamental and applied research. An atomic energy-level scheme convenient for laser confinement, cooling, and narrow-band excitation was explored in the ultraprecise Yb frequency standards for time measurements [1] and relativistic geodesy applications [2]. Yet further refinement has been predicted for a clock based on the Yb dimer [3]. Numerous photoassociation spectroscopy (PAS) studies on the degenerate Yb gases have led to significant insight into ultracold collision dynamics, long-range interactions, and exotic diatomic states [4–14]. A variety of naturally abundant isotopes with bosonic and fermionic natures made the Yb dimer very attractive for studying spectroscopic manifestations of nonclassical mass-dependent effects [11,15].

Particularly challenging is the use of PAS measurements to constrain short-range gravitylike forces at the nanometer scale to affirm and improve the results of neutron-scattering and atomic-force-microscopy experiments [16]. It has been shown that the unprecedented 0.5-kHz accuracy of the PAS data on the near-threshold rovibrational levels of Yb_2 is enough to improve existing constraints on the Yukawa-type forces [17,18] by almost two orders of magnitude. This, however, requires essential refinement of the underlying theoretical model for PAS spectroscopy.

The beyond-Born-Oppenheimer (BBO) model introduced in Ref. [11] relied on the Born-Oppenheimer (BO) reference, in which the *ab initio* potential for the Yb_2 ground $^1\Sigma_g^+(0_g^+)$ state [19] was used with the adjustable well-depth scaling parameter and the long-range tail. The BBO terms included were the adiabatic mass-dependent corrections [15,20] and isotopic field shift [15]. Initial approximations of each term were taken from different sources and also contained adjustable parameters. The best fits to the experimentally measured energies of 13 near-threshold levels of the bosonic isotopomers $^{168,170,174}Yb_2$ gave rms deviations around 113 kHz ($3.8 \times 10^{-6}\,cm^{-1}$) and 30 kHz ($1.0 \times 10^{-6}\,cm^{-1}$) for the reference BO and BBO models, respectively.

Despite this seemingly impressive agreement, theoretical rms deviations are 60 times larger than the experimental uncertainty. Taking into account a limited number of the levels probed experimentally and their predominant sensitivity to long-range interatomic interactions, a plausible way of refining the theory is to obtain more robust initial guesses for molecular parameters, although a more thorough elaboration of the nonadiabatic corrections and inclusion of subtle relativistic and quantum electrodynamic effects [16] by no means can be discarded. An obvious first step is the refinement of the BO Yb_2 potential, which contributes by far the major share of uncertainty and is not defined globally with suitable veracity [6,19,21–24].

Indeed, this potential is accurately defined only in the long-range region. The dispersion coefficients were the subject of reliable *ab initio* calculations [25–28]. In addition,

*giorgio.visentin@skoltech.ru
†a.buchachenko@skoltech.ru
‡ptecmer@fizyka.umk.pl

very high sensitivity of the ultracold data to the lowest-order C_6 and C_8 coefficients permitted their high-precision adjustment [6,11,21]. However, PAS and scattering length data are not sensitive enough to interatomic interaction at short and medium ranges. In terms of the semiclassical analysis by Gribakin and Flambaum [29], they can fix the area of the potential minimum but not its position R_e and depth D_e. The number of bound vibrational energy levels $N_{\max}$ is therefore known, and $N_{\max} = 72$ for the reference $^{174}Yb_2$ dimer was used to test the BO models [6,11,21]. Model potentials satisfying this condition with $R_e = 4.50$ Å and $D_e = 1083\,\mathrm{cm}^{-1}$ were able to fit the PAS data with an rms deviation of 54 kHz ($1.8 \times 10^{-6}\,\mathrm{cm}^{-1}$) [6,21], which is better than the BO model did, with the *ab initio* potential having $R_e = 4.55$ Å and D_e adjusted to $743\,\mathrm{cm}^{-1}$ (113 kHz cited above) [11]. Worse still, no room-temperature experimental data attesting to the Yb_2 potential minimum exist. An exception is the mass-spectrometric dissociation energy estimation of $1400 \pm 1400\,\mathrm{cm}^{-1}$ [30]. To that end, it is extremely important to provide a reliable *ab initio* electronic structure model for Yb_2 and fully understand its limitations.

Consistent *ab initio* treatment of all the effects physically important for the interaction of two Yb atoms is not feasible. The predominantly dispersion bonding character implies extensive recovery of the dynamic electron correlation, including the core-valence and outer-core correlations, in a highly saturated basis set heavily augmented with a diffuse component. The scalar-relativistic (SR) coupled-cluster method with singles, doubles, and noniterative triples [CCSD(T)] and extrapolation to the complete-basis-set (CBS) limit provide the only tractable means to meet these requirements. It disregards, however, essential contributions from high-order cluster excitations. Furthermore, vectorial relativistic effects, such as spin-orbit coupling (SOC), are not negligible for lanthanides [31]. To estimate them quantitatively, one should assess the SR results against the sophisticated four-component calculations, which are far more restrictive with regard to the basis-set size and extent of the correlation treatment. All of these factors together led to a considerable mismatch between the literature *ab initio* results for Yb_2 [19,22–24], which calls into question what should be considered as a reference. The first goal of the present work is therefore to address that challenge by performing the most reliable all-electron SR CCSD(T) calculations and assessing their convergence. Because it is performed within the conventional *ab initio* frames, our analysis is expected to be useful for similar dispersion-bound molecules containing lanthanide atoms. The second goal is to provide improved representation of the global BO Yb_2 potential with its preliminary uncertainty estimation. We thus describe the semiclassical scaling of the CCSD(T) potentials to make a preliminary assessment of their compliance with the ultracold data, explore the sensitivity to the parameters of the potential minimum, and estimate the BO contributions not included in the *ab initio* calculations. On the one hand, our results support the previous BO and BBO models [11,16]; on the other hand, they provide a more reliable and flexible reference BO potential function for use in the more sophisticated BO and BBO spectroscopic models.

The next section combines detailed descriptions of the *ab initio* approaches and results. The high degree of technicality is indispensable to make sure that our findings are reproducible and transferable. In Sec. II C, we present the results of the semiclassical analysis of the *ab initio*–based global BO potential and discuss their implications for BO and BBO modeling. Our conclusions follow.

II. *AB INITIO* CCSD(T) CALCULATIONS

A. Scalar-relativistic calculations with MOLPRO

The CCSD(T) calculations were performed using the exact two-component (X2C) scalar-relativistic Hamiltonian [32–37] as realized in the MOLPRO 2015.1 program package [38]. In all our calculations the energy convergence threshold was set to $10^{-10}E_h$. The sequence of the correlation-consistent polarized valence n zeta (cc-pVnZ) basis sets with cardinal numbers n = D, T, Q (hereinafter VnZ for brevity) contracted for use with the X2C approximation [39] was used. To compensate for the lack of optimized diffuse augmentation in the cc-pVnZ sets, we added one or two primitives for each symmetry type, with the exponents continuing the sequence of basis exponents in an even-tempered manner with the default parameters of the MOLPRO package. In what follows, these options are denoted as e1 and e2, respectively. The $3s3p2d2f1g$ set of bond functions (bf) [40] placed at the midpoint of the Yb-Yb distance was also used for the same purpose. The calculations were performed in the D_{2h} symmetry group for the dimer and the C_{2v} group for the Yb atom in the full dimer basis to implement the counterpoise (CP) correction [41] using the restricted Hartree-Fock reference functions. Two series of the CCSD(T) calculations correlated $5s$, $5p$, $4f$, and $6s$ orbitals (the c46 option, with 46 electrons within the core per atom) and $4s$, $4p$, and $4d$ orbitals (the c28 option). A negligible effect of correlating deeper shells (orbitals below $4s$) on the potential-energy-well parameters and dispersion coefficients of the dimer was proven in Refs. [24,28]. We should also note in this regard that we encountered difficulty with convergence when using the correlation-consistent polarized weighted core-valence basis sets (cc-pwCVnZ) with $n > 2$. Thus, the results for that basis-set family, which is more appropriate for the c28 correlation option, are not reported. The counterpoised potentials obtained with the VDZ, VTZ, and VQZ basis sets were extrapolated to the CBS limit using the mixed exponential-Gaussian formula [42,43].

A nonuniform grid of 57 internuclear distances spanning the range from 2 to 50 Å was used. At distances longer than 25 Å, erratic nonsmooth variations of energies were detected. This prevents a firm determination of the dominant C_6 dispersion coefficient by fitting and limits the accuracy of interaction energies by $0.05\,\mathrm{cm}^{-1}$. The Supplemental Material [44] tabulates the potential energies obtained with each VnZ basis set extrapolated to the CBS limit.

To establish the connection to the relativistic calculations with the DIRAC code described in the next section, a few auxiliary X2C CCSD(T) calculations were performed on a slightly shorter grid. They used the c48 correlation option ($5p$, $4f$, and $6s$ orbitals correlated) and the original VDZ, uncontracted VDZ (uVDZ), and uncontracted Dyall double-ζ [45] bases, all without further augmentation.

TABLE I. Parameters of the CCSD(T) c48 potentials calculated with the double-ζ basis sets. Calculations with DIRAC used the Gaussian nuclear model unless stated otherwise.

Method	Package	σ (Å)	R_e (Å)	D_e (cm^{-1})
X2C VDZ	MOLPRO	4.080	4.741	475.4
X2C uVDZ	MOLPRO	4.062	4.727	478.0
X2C Dyall	MOLPRO	4.022	4.694	531.9
SF-X2C Dyall point charge	DIRAC	4.022	4.694	531.9
SF-X2C Dyall	DIRAC	4.018	4.692	533.0
SF-DC Dyall	DIRAC	4.024	4.694	526.0
4C-DC Dyall	DIRAC	4.012	4.686	532.3

B. Assessment of the scalar-relativistic approximation with DIRAC

All the CCSD(T) calculations were carried out using the DIRAC19 relativistic software package [46] and utilized a linear $D^*_{\infty h}$ symmetry, the valence double-ζ basis set of Dyall [45], and the Gaussian nuclear model, if not stated otherwise. The calculations kept $4f$, $5p$, and $6s$ spinors (orbitals) correlated (leaving 48 inner electrons within the core per atom, the c48 option), and all virtuals were active.

We assessed the performance of various relativistic Hamiltonians. Specifically, these include (i) the four-component Dirac-Coulomb Hamiltonian (with a default setup [47]), denoted as 4C-DC; (ii) the spin-free Dirac-Coulomb Hamiltonian, denoted as SF-DC [48]; and (iii) the spin-free X2C Hamiltonian [32–37], denoted as SF-X2C. An additional set of calculations was performed for the SF-X2C Hamiltonian with the point-charge nuclear model. That allowed for direct comparison with the SR calculations carried out in the MOLPRO software package described above.

As we aimed to analyze the relativistic effects on the equilibrium parameters, the grid of 27 internuclear distances R was restricted to $5a_0$–$20a_0$ (roughly 2.6–10.6 Å) interval. The CP correction [41] was applied by imposing the $C^*_{\infty v}$ point-group symmetry. Tabulated *ab initio* potential energies with different relativistic Hamiltonians are available in the Supplemental Material [44].

Table I compares the parameters of the CCSD(T) c48 Yb_2 interaction potentials, namely, the inflection point at zero kinetic energy σ and equilibrium parameters R_e and D_e, as obtained for the basis sets of double-ζ quality without further augmentations. Implementations of the X2C Hamiltonian in the DIRAC and MOLPRO packages gave identical results for the Dyall basis set. The MOLPRO calculations with the cc-pVnZ-type basis showed a weaker bonding. This indicates that the VDZ basis, even in its uncontracted form, is not optimal for the predominantly dispersion interaction we are dealing with here. The contraction alters D_e marginally but reduces R_e by almost 0.02 Å. Such a significant increment should persist for the VnZ sets of higher cardinal numbers and thus cannot be recovered by extrapolation to the CBS limit. The calculations with the DIRAC package demonstrated that a slight increase in the binding energy due to SOC and finite-nuclei effects is nearly canceled for the SF X2C Hamiltonian. By contrast, the related contraction of R_e by 0.01 Å reflects the main deficiency of the scalar-relativistic approximation.

TABLE II. Parameters of the present extrapolated X2C CCSD(T) Yb_2 potentials and those from literature.

Method	σ (Å)	R_e (Å)	D_e (cm^{-1})	$\mathcal{N}$
VnZ c46	3.916	4.593	617.5	66.99
VnZe1 c46	3.907	4.596	646.1	68.15
VnZe2 c46	3.907	4.598	646.9	68.20
VnZbf c46	3.906	4.594	654.6	68.35
VnZ c28	3.915	4.590	615.0	66.90
VnZe1 c28	3.906	4.596	643.6	68.12
VnZbf c28	3.896	4.585	657.5	68.54
ANO-RCC c28 [24]		4.665	580	
ECP28MWB [19]	3.870	4.522	723.7	70.97
ECP28MWB [22]		4.549	742	
28e GRECP+OC [23]		4.683	642	
28e GRECP+OC+iTQ [23]		4.615	767	
28e GRECP+OC+iTQ+SOC [23]		4.582	787	

C. Convergence of the scalar-relativistic results

To assess the convergence of the Yb_2 X2C CCSD(T) calculations with respect to the diffuse basis augmentation and the core-correlation treatment it is instructive to analyze the results at the CBS limit, which accounts for the convergence with respect to the cardinal number of the primary basis set. As the CBS extrapolation procedure cannot be rigorously defined, it introduces additional uncertainty [42,43,49–54]. Moreover, additional ambiguity might originate from the CBS extrapolation of the basis-set sequences augmented with bond functions. This quite technical issue is discussed in the Supplemental Material.

Table II lists the values of the interaction-potential parameters after the CBS extrapolation and the semiclassical estimates of the number of bound vibrational energy levels $\mathcal{N}$ obtained with the potential model introduced in this section (see below).

The difference between the c46 and c28 calculations (all else being equal) indicates that the correlation of the $4s4p4d$ shells reduces the bonding of Yb atoms to a minor extent. That is in line with the previous calculations for the Yb_2 potential [24]. Diffuse augmentation is essential to better recover the dispersion interactions. While involving the atom-centered even-tempered diffuse primitives (e1) is suboptimal, it still results in good convergence that follows from the marginal effect of including the second primitive set (e2). The addition of the bond functions enhances Yb_2 bonding to a larger extent. For this reason and for smaller CBS uncertainty due to faster convergence with the cardinal basis number, we took the present VnZbf c28 result as the reference to estimate the converged X2C CCSD(T) potential parameters as $R_e = 4.585 \pm 0.01$ Å and $D_e = 658 \pm 15\,\text{cm}^{-1}$, where the major share of uncertainties belongs to the form of diffuse augmentation and the minor share belongs to the CBS extrapolation. The deviation between the X2C CCSD(T) calculations with the cc-pVnZ-type and Dyall-type basis sets discussed in Sec. II B creates an additional source of uncertainty. To estimate it better, we consider an artificial CBS extrapolation of the SF-X2C CCSD(T) results for the Dyall VDZ basis set with extrapolation coefficients taken from the corresponding X2C CCSD(T)

VnZ c48 series. It results in $R_e \approx 4.54$ Å and $D_e \approx 670\,\mathrm{cm}^{-1}$ or ≈4.53 Å and ≈700 cm^{-1} if the increments due to diffuse function augmentation are added. Because the physical origin of such a significant mismatch is not clear, the latter values can be taken only as an indication that the present calculations likely underestimate the bonding of Yb atoms at the CCSD(T) level of theory.

The results of the previous SR CCSD(T) calculations are presented in Table II as well. The only available all-electron calculations from Ref. [24] underestimate the present D_e values by around 10% and overestimate R_e by 0.07 Å. Besides the minor difference in the applied scalar-relativistic Hamiltonians (X2C vs Douglas-Kroll-Hess of the second order), this mismatch is likely due to the lack of diffuse functions in the atomic natural orbital relativistic semicore correlation (ANO-RCC) basis set and the absence of the CP correction. Even though the ANO-RCC basis set was designed to correlate Yb orbitals starting from the 5s shell, the correlation of deeper shells did not result in any problems as reported in Ref. [24]. The best ANO-RCC estimation falls between the present VTZe1 and VQZ results, despite the fact that the ANO-RCC basis set was used in its uncontracted form.

The potential from Refs. [19] is based on the small-core effective core potential ECP28MWB [55] combined with the corresponding ANO basis set [56] augmented by the specially designed atom-centered diffuse function set [57] and the bf set [40] simultaneously. It implies stronger bonding of Yb atoms than the present series does; namely, the binding energy is larger by 11%, and the equilibrium distance is shorter by 1.5%. This difference should be attributed to the uncertainties of the effective-core-potential description of the inner shells and of the quality of the ANO basis, as corroborated by the calculations by Cao and Dolg with the same basis but different diffuse augmentation [22]. Mosyagin and coworkers [23] investigated the bonding of Yb atoms using the 28-electron generalized relativistic effective core potential (GRECP) and a series of supplementary basis sets. Only four outer 6s electrons were correlated in their reference CCSD(T) calculations with the largest basis. Correction to outer core correlation (OC, equivalent to the present c46 core option) was evaluated with a smaller basis. At this level, their result for binding energy almost falls within the error bars we predicted, but the equilibrium distance is strongly overestimated.

To go beyond the X2C CCSD(T) approximation, one should consider the vectorial relativistic effects and contributions from the higher-order cluster excitation. For the former, we can use the present 4C-DC calculations. Table I indicates that for the double-ζ basis, the main effect with respect to the X2C approximation is the contraction of the dimer bond length. Artificial CBS extrapolation with the coefficients derived from the X2C CCSD(T) VnZ c48 series infers the shrinkage of R_e by 0.01 Å and an increase of D_e by $9\,\mathrm{cm}^{-1}$. Reference [23] reported a correction twice as large (Table II, labeled "+SOC"), but the quasirelativistic two-component density-functional theory employed therein is certainly much less accurate. Mosyagin *et al.* [23] provided the only (indirect) estimation for the higher-order cluster corrections. Iterative contributions of triples and quadruples were recovered by subtracting CCSD(T) energy from the full configuration-interaction energy, both obtained by correlating four outer electrons in a medium-size basis set, labeled "+iTQ" in Table II. The effect, a 1.5% reduction of R_e and 20% increase of D_e, is quite significant. However, it is not possible to guess how it would behave upon expanding the basis set and the depth of the shells included in the correlation treatment.

Adding the present estimate for SOC and the iTQ correction from Ref. [23] to the converged X2C results cited above, we obtain $R_e \approx 4.45$ Å and $D_e \approx 825\,\mathrm{cm}^{-1}$ as a guess for the true Yb_2 BO potential. Uncertainties of these values are hard to quantify, but they are likely not less than 0.1 Å and $100\,\mathrm{cm}^{-1}$, respectively.

III. GLOBAL BO POTENTIAL BY SEMICLASSICAL SCALING

As was already mentioned, PAS and scattering length measurements established the number of the bound vibrational levels $N_{\max}$ of the Yb_2 dimer. Previous analysis indicated that this condition can be applied to the BO potentials, as the BBO contributions are too small to alter the number of levels [11].

To test the present *ab initio* results, we accepted the semianalytical representation of the global BO potential $V(R)$ introduced in Ref. [11]:

$$V(R) = [1 - f(R)]sV_{\mathrm{SR}}(R) + f(R)V_{\mathrm{LR}}(R), \tag{1}$$

where the *ab initio* points interpolated by cubic splines stand for the short-range part V_{SR} and the long-range part contains the two lowest dispersion-interaction terms,

$$V_{\mathrm{LR}}(R) = -C_6/R^6 - C_8/R^8, \tag{2}$$

as the PAS data are not sensitive to the next C_{10} term [11]. The switching function has the fixed form

$$f(R) = \begin{cases} 0 & \text{if } R \leqslant a, \\ \frac{1}{2} + \frac{1}{4}\sin\frac{\pi x}{2}\left(3 - \sin^2\frac{\pi x}{2}\right) & \text{if } a < R < b, \\ 1 & \text{if } R > b, \end{cases} \tag{3}$$

with $x = [(R-a) + (R-b)]/(b-a)$, $a = 10a_0$ (5.292 Å), $b = 19a_0$ (10.054 Å). The values of the dispersion coefficients $C_6 = 1937.27$ and $C_8 = 226517$ a.u. were taken as fitted in Ref. [11] and were kept fixed. The scaling parameter s is adjustable. If $s = 1$, Eq. (1) describes the interpolation of the original *ab initio* points at $R \leqslant a$.

The number of bound vibrational levels was obtained semiclassically following the procedure described in Ref. [29]. The semiclassical phase at zero kinetic energy is given by

$$\Phi = \frac{1}{\hbar}\int_{\sigma}^{\infty} \sqrt{2\mu[-V(R)]}dR, \tag{4}$$

where μ is the reduced mass of the Yb dimer, for which we used the atomic reduced mass of the $^{174}Yb_2$ dimer. Note that Eqs. (1) and (3) permit analytical integration of the phase from $R = b$ to infinity, which greatly facilitates an accurate numerical evaluation of the integral (4). Then $N_{\max} = [\mathcal{N}]$, with $\mathcal{N} = \Phi/\pi + 3/8$. The $\mathcal{N}$ values for the original ($s = 1$) X2C CCSD(T) potentials are given in Table II. The best ones consistently support 68 bound levels.

Next, we vary parameter s until $\mathcal{N}$ exceeds 72 to get $s_{\min}$ and until $\mathcal{N}$ remains less than 73 to get $s_{\max}$. The resulting

TABLE III. Scaling dimensionless factors s and binding energies (cm^{-1}) of the X2C CCSD(T) potentials for the $^{174}Yb_2$ dimer.

Potential	s_{min}	$s_{min}D_e$	s_{max}	$s_{max}D_e$	mean D_e
VnZ c46	1.233	761.4	1.281	791.0	776 ± 15
VnZe1 c46	1.172	757.2	1.218	786.9	772 ± 15
VnZe2 c46	1.170	757.2	1.215	786.0	772 ± 15
VnZbf c46	1.162	760.6	1.208	790.7	776 ± 15
VnZ c28	1.238	761.4	1.286	790.9	776 ± 15
VnZe1 c28	1.174	755.6	1.219	784.5	770 ± 15
VnZbf c28	1.153	758.0	1.198	787.7	773 ± 15

values of s, scaled binding energies, and mean binding energies computed with the X2C CCSD(T) V_{SR} potentials are listed in Table III. First, it is evident that the constraint on the bound level projects the original potentials, whose binding energies vary by $43\,cm^{-1}$, to much narrower intervals of $6\,cm^{-1}$ for the limiting and mean values. Such mapping reflects the similarity in the overall shapes of the attractive potentials calculated using the different *ab initio* schemes. Second, the variations of D_e values that obey the constraint is $30\,cm^{-1}$. As follows from the numerical solutions of the vibrational Schrödinger equation, the position of the last near-threshold $N_{max} - 1 = 71$ level in the same range of s varies by around $0.02\,cm^{-1}$. It gives a clue that uncertainty in fixing the near-threshold levels (e.g., by PAS data) increases by three orders of magnitude upon propagation to the equilibrium properties.

The preceding analysis of the *ab initio* results points out that X2C CCSD(T) CBS calculations significantly overestimate the dimer equilibrium distance. The shift of the potential towards a shorter range should obviously affect the scaling by increasing the phase Φ. To take this uncertainty into account, we introduced the shift parameter d and replaced the *ab initio* part of the model function (1) by the shifted potential $V_{SR}(R - d)$. For each $d \in [-0.02, 0.14]$ the limiting scaling parameters s_{min} and s_{max} were found using the same criteria as above. Figure 1 shows the results in terms of shifted and scaled equilibrium parameters for the VnZbf c28 *ab initio* potential. The position and mean depth of the potential well are correlated linearly with the coefficient $200 \pm 1\ cm^{-1}/Å$. The limits of D_e variation weakly depend on d and amount to $\pm 15\,cm^{-1}$. If we add the uncertainty of the scaled dissociation energies from Table III, the margins expand to $\pm 18\,cm^{-1}$. Figure 1 also shows the result from Ref. [11], where the ECP28MWB potential [19] was used as the reference. It lies on the extended lower bound of the present calculations. We believe that Fig. 1 identifies the most likely ranges for equilibrium parameter variations, i.e., $R_e \in [4.45, 4.55]$ Å and $D_e = 755 \pm 20\,cm^{-1}$.

Another implication of the present analysis is the possibility to replace the model function (1) with a more flexible form,

$$V(R) = [1 - f(R)]s(d)V_{SR}(R - d) + f(R)V_{LR}(R), \qquad (5)$$

where the constraint $s(d) = -0.304d + 1.176$ results from the correlation between D_e and R_e and V_{SR} is the present X2C CCSD(T) VnZbf c28 pointwise potential, whereas Eqs. (2) and (3) and their parameters remain unchanged. Keeping a single adjustable parameter [d instead of s in Eq. (1)], the new function features a sensitivity to both the position and depth of the potential minimum and thus should have better properties for accurate BO or BBO fitting of the PAS data.

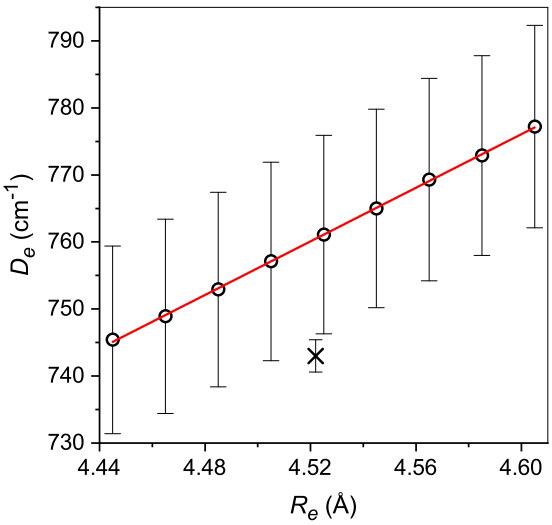

FIG. 1. Correlation of the scaled binding energy and shifted equilibrium distance of the Yb_2 interaction potential based on the *ab initio* VnZbf c28 data. Solid lines represents the linear fit. The cross indicates the scaled Born-Oppenheimer result from Ref. [11].

IV. CONCLUSIONS

The present calculations set the scalar-relativistic CCSD(T) benchmark for the ground-state potential of the Yb dimer. Achieving the convergence with respect to the basis-set saturation and the extent of the core-correlation treatment, we estimated its equilibrium parameters as $R_e = 4.585 \pm 0.01$ Å and $D_e = 658 \pm 15\,cm^{-1}$ and explained the main sources of disagreements in the previous *ab initio* calculations. The first four-component relativistic CCSD(T) calculations performed with a double-ζ basis generally support the validity of the X2C approximation but pointed to bond length shrinkage of about 0.01 Å as the main effect caused by relativistic contraction. The quoted uncertainties, not exceeding 3%, can be narrowed down only by customizing the basis set for the Yb atom and/or the bond function for the Yb_2 molecule. The design principle of general-purpose bases may well be suboptimal for the particular system considered and the accuracy level required.

The X2C CCSD(T) potentials were used to approximate the BO Yb_2 potential represented by the model semianalytical function. On the one hand, semiclassical scaling to the known number of bound vibrational levels reduces the uncertainty in Yb_2 binding energy by almost an order of magnitude. This indicates that variations of the *ab initio* computational scheme alter the shape of the bound potential insignificantly. On the other hand, the constraint on the number of bound levels has its own uncertainty of the same order ($30\,cm^{-1}$, or 4%) as that of initial *ab initio* potential. It reflects the weak sensitivity of the ultracold PAS data to the potential minimum parameters. We found that the quoted uncertainty for D_e is three orders of magnitude larger than the uncertainty in the position of the last bound vibrational level.

We also analyzed the effect of uncertainty on the equilibrium distance established in the *ab initio* calculations. As a result, we bound the potential parameters of the BO Yb_2 potential as $R_e \in [4.45, 4.55]$ Å and $D_e \in [735, 775]\,\mathrm{cm}^{-1}$. This supports the reliability of the previous BO fit to PAS data made with the potential having $R_e = 4.52$ and optimized $D_e = 743.0 \pm 2.4\,\mathrm{cm}^{-1}$ [11]. We suggested modifying the model BO potential function to account for strong correlation of the position and depth of the potential well.

Finally, we should stress that the sophisticated BO fit to PAS data [11] was able to reduce uncertainty in the D_e value from 20 to $2\,\mathrm{cm}^{-1}$ to ensure 4×10^{-6} rms deviation from the measured energies of the near-threshold levels. Thus, the model function and its uncertainty obtained here promise remarkable improvements of the above-mentioned fits.

ACKNOWLEDGMENTS

We thank M. Borkowski, P. Żuchowski, and D. Kędziera for many helpful discussions. Financial support from the Russian Science Foundation under Project No. 17-13-01466 is gratefully acknowledged. P.T. acknowledges an OPUS 17 research grant from the National Science Centre, Poland (Grant No. 2019/33/B/ST4/02114), and a scholarship for outstanding young scientists from the Ministry of Science and Higher Education.

[1] A. D. Ludlow, M. M. Boyd, J. Ye, E. Peik, and P. O. Schmidt, Rev. Mod. Phys. **87**, 637 (2015).
[2] W. F. McGrew, X. Zhang, R. J. Fasano, S. A. Schaeffer, K. Beloy, D. Nicolodi, R. C. Brown, N. Hinkley, G. Milani, M. Schioppo, T. H. Yoon, and A. D. Ludlow, Nature (London) **564**, 87 (2018).
[3] M. Borkowski, Phys. Rev. Lett. **120**, 083202 (2018).
[4] S. Tojo, M. Kitagawa, K. Enomoto, Y. Kato, Y. Takasu, M. Kumakura, and Y. Takahashi, Phys. Rev. Lett. **96**, 153201 (2006).
[5] K. Enomoto, M. Kitagawa, S. Tojo, and Y. Takahashi, Phys. Rev. Lett. **100**, 123001 (2008).
[6] M. Borkowski, R. Ciuryło, P. S. Julienne, S. Tojo, K. Enomoto, and Y. Takahashi, Phys. Rev. A **80**, 012715 (2009).
[7] Y. Takasu, Y. Saito, Y. Takahashi, M. Borkowski, R. Ciuryło, and P. S. Julienne, Phys. Rev. Lett. **108**, 173002 (2012).
[8] S. Kato, S. Sugawa, K. Shibata, R. Yamamoto, and Y. Takahashi, Phys. Rev. Lett. **110**, 173201 (2013).
[9] D. G. Green, C. L. Vaillant, M. D. Frye, M. Morita, and J. M. Hutson, Phys. Rev. A **93**, 022703 (2016).
[10] Y. Takasu, Y. Fukushima, Y. Nakamura, and Y. Takahashi, Phys. Rev. A **96**, 023602 (2017).
[11] M. Borkowski, A. A. Buchachenko, R. Ciuryło, P. S. Julienne, H. Yamada, Y. Kikuchi, K. Takahashi, Y. Takasu, and Y. Takahashi, Phys. Rev. A **96**, 063405 (2017).
[12] L. Franchi, L. F. Livi, G. Cappellini, G. Binella, M. Inguscio, J. Catani, and L. Fallani, New J. Phys. **19**, 103037 (2017).
[13] R. Bouganne, M. B. Aguilera, A. Dareau, E. Soave, J. Beugnon, and F. Gerbier, New J. Phys. **19**, 113006 (2017).
[14] G. Cappellini, L. F. Livi, L. Franchi, D. Tusi, D. Benedicto Orenes, M. Inguscio, J. Catani, and L. Fallani, Phys. Rev. X **9**, 011028 (2019).
[15] J. J. Lutz and J. M. Hutson, J. Mol. Spectrosc. **330**, 43 (2016).
[16] M. Borkowski, A. A. Buchachenko, R. Ciuryło, P. S. Julienne, H. Yamada, Y. Kikuchi, Y. Takasu, and Y. Takahashi, Sci. Rep. **9**, 14807 (2019).
[17] P. Fayet, Classical Quantum Gravity **13**, A19 (1996).
[18] E. G. Adelberger, J. H. Gundlach, B. R. Heckel, S. Hoedl, and S. Schlamminger, Prog. Part. Nucl. Phys. **62**, 102 (2009).
[19] A. A. Buchachenko, G. Chałasiński, and M. M. Szcześniak, Eur. Phys. J. D **45**, 147 (2007).
[20] K. Pachucki and J. Komasa, J. Chem. Phys. **129**, 034102 (2008).
[21] M. Kitagawa, K. Enomoto, K. Kasa, Y. Takahashi, R. Ciuryło, P. Naidon, and P. S. Julienne, Phys. Rev. A **77**, 012719 (2008).
[22] X. Cao and M. Dolg, Mol. Phys. **101**, 1967 (2003).
[23] N. S. Mosyagin, A. N. Petrov, and A. V. Titov, Int. J. Quantum Chem. **111**, 3793 (2010).
[24] P. Tecmer, K. Boguslawski, M. Borkowski, P. S. Żuchowski, and D. Kedziera, Int. J. Quantum Chem. **119**, e25983 (2019).
[25] P. Zhang and A. Dalgarno, Mol. Phys. **106**, 1525 (2008).
[26] M. S. Safronova, S. G. Porsev, and C. W. Clark, Phys. Rev. Lett. **109**, 230802 (2012).
[27] S. G. Porsev, M. S. Safronova, A. Derevianko, and C. W. Clark, Phys. Rev. A **89**, 012711 (2014).
[28] G. Visentin and A. A. Buchachenko, J. Chem. Phys. **151**, 214302 (2019).
[29] G. F. Gribakin and V. V. Flambaum, Phys. Rev. A **48**, 546 (1993).
[30] M. Guido and G. Balducci, J. Chem. Phys. **57**, 5611 (1972).
[31] P. Pyykkö, Chem. Rev. **88**, 563 (1988).
[32] D. Kędziera, in *Recent Progress in Computational Sciences and Engineering*, Lecture Series on Computer and Computational Sciences Vol. 7A–B (Brill Academic Publishers, Leiden, 2006), pp. 252–255.
[33] D. Kędziera and M. Barysz, Chem. Phys. Lett. **446**, 176 (2007).
[34] M. Iliaš and T. Saue, J. Chem. Phys. **126**, 064102 (2007).
[35] J. Sikkema, L. Visscher, T. Saue, and M. Ilias, J. Chem. Phys. **131**, 124116 (2009).
[36] W. Liu and D. Peng, J. Chem. Phys. **131**, 031104 (2009).
[37] D. Peng and M. Reiher, Theor. Chem. Acc. **131**, 1081 (2012).
[38] H.-J. Werner, P. J. Knowles, G. Knizia, F. R. Manby, and M. Schütz, Wiley Interdiscip. Rev.: Comput. Mol. Sci. **2**, 242 (2012).
[39] Q. Lu and K. A. Peterson, J. Chem. Phys. **145**, 054111 (2016).
[40] S. M. Cybulski and R. R. Toczyłowski, J. Chem. Phys. **111**, 10520 (1999).
[41] S. Boys and F. Bernardi, Mol. Phys. **19**, 553 (1970).
[42] K. A. Peterson, D. E. Woon, and T. H. Dunning, Jr., J. Chem. Phys. **100**, 7410 (1994).
[43] D. Feller and J. A. Sordo, J. Chem. Phys. **112**, 5604 (2000).
[44] See Supplemental Material at http://link.aps.org/supplemental/10.1103/PhysRevA.104.052807 for description of the complete

basis set extrapolation procedures and tabulated *ab initio* potentials.

[45] A. S. P. Gomes, K. G. Dyall, and L. Visscher, Theor. Chem. Acc. **127**, 369 (2010).

[46] T. Saue, R. Bast, A. S. P. Gomes, H. J. A. Jensen, L. Visscher, I. A. Aucar, R. Di Remigio, K. G. Dyall, E. Eliav, E. Fasshauer, T. Fleig, L. Halbert, E. D. Hedegård, B. Helmich-Paris, M. Iliaš, C. R. Jacob, S. Knecht, J. K. Laerdahl, M. L. Vidal, M. K. Nayak, M. Olejniczak, J. M. Haugaard Olsen, M. Pernpointner, B. Senjean, A. Shee, A. Sunaga, and J. N. P. van Stralen, J. Chem. Phys. **152**, 204104 (2020).

[47] L. Visscher, Theor. Chem. Acc. **98**, 68 (1997).

[48] K. G. Dyall, J. Chem. Phys. **100**, 2118 (1994).

[49] J. M. L. Martin, Chem. Phys. Lett. **259**, 679 (1996).

[50] J. M. L. Martin and P. R. Taylor, J. Chem. Phys. **106**, 8620 (1997).

[51] D. Feller, J. Chem. Phys. **96**, 6104 (1992).

[52] D. Feller and K. A. Peterson, J. Chem. Phys. **108**, 154 (1998).

[53] M. P. de Lara-Castells, R. V. Krems, A. A. Buchachenko, G. Delgado-Barrio, and P. Villarreal, J. Chem. Phys. **115**, 10438 (2001).

[54] D. Feller, K. A. Peterson, and J. G. Hill, J. Chem. Phys. **135**, 044102 (2011).

[55] M. Dolg, H. Stroll, and H. Preuss, J. Chem. Phys. **90**, 1730 (1989).

[56] X. Cao and M. Dolg, J. Chem. Phys. **115**, 7348 (2001).

[57] A. A. Buchachenko, G. Chałasiński, and M. M. Szcześniak, Struct. Chem. **18**, 769 (2007).